

PACS numbers: 33.50.–j; 33.70.–w; 73.22.–f
DOI: 10.1070/QE2015v045n10ABEH015791

Influence of silver nanoparticles on relaxation processes and efficiency of dipole–dipole energy transfer between dye molecules in polymethylmethacrylate films

V.V. Bryukhanov, E.I. Konstantinova, R.Yu. Borkunov, M.V. Tsarkov, V.A. Slezhkin

Abstract. **The fluorescence and phosphorescence of dyes in thin polymethylmethacrylate (PMMA) films in the presence of ablated silver nanoparticles has been investigated in a wide temperature range by methods of femtosecond and picosecond laser photoexcitation. The fluorescence and phosphorescence times, as well as spectral and kinetic characteristics of rhodamine 6G (R6G) molecules in PMMA films are measured in a temperature range of 80–330 K. The temperature quenching activation energy of the fluorescence of R6G molecules in the presence of ablated silver nanoparticles is found. The vibrational relaxation rate of R6G in PMMA films is estimated, the efficiency of the dipole–dipole electron energy transfer between R6G and brilliant green molecules (enhanced by plasmonic interaction with ablated silver nanoparticles) is analysed, and the constants of this energy transfer are determined.**

Keywords: *ablation, silver nanoparticles, rhodamine 6G, polymethylmethacrylate films, dipole–dipole transfer, plasmon resonance, 'hot' fluorescence, femtosecond photoexcitation, low temperatures, β-relaxation.*

1. Introduction

Local surface plasmon resonance (LSPR) is of great interest for researchers and technologists in view of its potential for nanophotonics [1], hybrid and polymer photovoltaic converters [2], optoelectronic devices and sensors [3, 4] and dipole nanolasers with nanoantennas [5].

One of the most important fields of research in optical nanophotonics is the use of polymer materials as matrices for phosphors; quantum dots; luminescent complexes of rare-earth elements; and other luminescent complexes, involved in electron energy transfer and conversion processes in various practical applications. For example, silver ions can be implanted into polymer matrices [6] to form a metal nanophase, in which LSPR occurs. Highly sensitive emergency sensors have been designed by introducing metal nanoparticles into optical fibres [7]. Having introduced silver or gold nanoparticles into a vitrified polymer, one can increase the electron energy transfer efficiency [8, 9] or use polymethylmethacrylate (PMMA) polymer films with metal nanoparticles and phosphor molecules in solar energy concentrators [10, 11]. At the same time, introducing metal nanoparticles in the form of sols into a polymer, one can change not only optical properties of a polymer film but also its structural and relaxation properties.

In this paper, we report the results of studying PMMA films containing dyes [rhodamine 6G (R6G) and brilliant green (BG)] and silver nanoparticles, obtained by laser ablation in liquid, using spectral and kinetic methods in a wide temperature range.

V.V. Bryukhanov, R.Yu. Borkunov, M.V. Tsarkov Immanuel Kant Baltic Federal University, ul. Nevskogo 14, 236041 Kaliningrad, Russia; e-mail: bryukhanov_v.v@mail.ru;
E.I. Konstantinova, V.A. Slezhkin Kaliningrad State Technical University, Sovetskii prosp. 1, 236022 Kaliningrad, Russia; e-mail: konstantinovaeliz@gmail.com

Received 24 February 2015; revision received 12 April 2015
Kvantovaya Elektronika **45** (10) 908–913 (2015)
Translated by Yu.P. Sin'kov

2. Experimental

R6G and BG dyes were chosen as objects of study because of the strong overlap of their fluorescence and absorption spectra. Polymethylmethacrylate films were prepared by coating a glass surface with chloroform solutions containing dyes and PMMA of analytical grade. After drying at room temperature, the film thickness was $d \approx 40$ μm. The R6G concentrations in the films were $C = 3.1\times10^{-3}$ and 5×10^{-4} M; the BG concentrations were 7.8×10^{-4} and 1.6×10^{-4} M.

Silver nanoparticles were formed for 8 min by laser ablation of a polished silver plate in chloroform. We used a TETA-25 femtosecond laser equipped with a compressor (Avesta, Russia) (pulse duration $\tau = 280$ and 30 fs with a compressor switched off and switched on, respectively, and maximum pulse energy $W = 240$ μJ at a wavelength $\lambda = 1064$ nm).

The pulse repetition rate and number of pulses were programmed using a computer. The chloroform volume V in the cell with a target was 2.5 mL and the thickness of the liquid layer above the silver plate surface was $l = 3$ mm. The colloidal solution of ablated nanoparticles (ANPs) was stable for four weeks. The silver ANP concentration in the solution after ablation was $C_0 = 0.85\times10^{-9}$ M. Dyes and PMMA were added to the ANP-containing solution, after which the latter was deposited on a glass surface. The fluorescence spectra of molecules and fluorescence times were measured using a Fluorolog-3 optical modular system (Horiba, France). Fluorescence of dye molecules in PMMA films in this system was excited by a pulsed picosecond NanoLed laser diode ($\lambda = 508$ nm, $\tau < 200$ ps), emitting in the absorption band of R6G molecules. The fluorescence times were measured by a TCSPC photon counting module (Horiba, France) with an error of 3%–4% for a sample of three or four different dye-containing PMMA films. Femtosecond photoexcitation of dye molecules in the films was performed using a specially developed setup (Fig. 1). The error in measuring the fluorescence time on this setup was 4%–5%. Absorption spectra were recorded on a two-beam Shimadzu UV-2600 spectrophotometer (Japan)

in the range of 300–700 nm. Low-temperature spectral and kinetic measurements of the fluorescence and phosphorescence of PMMA films with R6G dye were performed upon femtosecond photoexcitation (λ = 516 nm) in an automatic low-temperature Optistat DN2-V nitrogen cryostat (Oxford Instruments, England) and upon excitation by a cw LCS-DTL-317 laser (Laser-Export Co. Ltd., Russia) (λ = 532 nm, P = 20–25 mW). Luminescence spectra were analysed by an ML44 monochromator (Solar Laser Systems, Belarus) equipped with an H10720-110 photoelectron multiplier (PEM) (Hamamatsu; Δt < 0.5 ns). The error in measuring spectra was $\Delta\lambda \approx 0.2$ nm. Luminescence oscillograms were recorded with a Tektronix DPO4104B oscilloscope (Δt < 0.35 ns). Silver ANP sizes were determined using a Photocor-Complex photon correlation system (Russia). The relative error in measuring the nanoparticle size was ~10%.

3. Results

Figure 1 shows a schematic diagram of an original, completely automatic fluorescent system based on femtosecond and cw lasers with a low-temperature nitrogen cryostat; this diagram demonstrates the specific features of operation of the femtosecond laser complex.

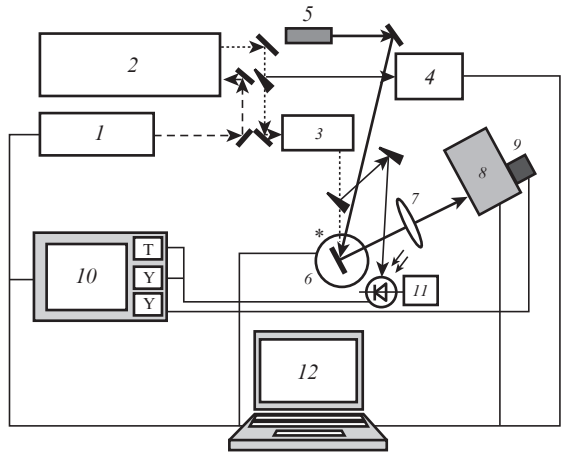

Figure 1. Schematic of the experimental setup: (*1*) femtosecond pulse generator TETA-25 (f = 20 kHz, Avesta, Russia); (*2*) femtosecond pulse compressor Compulse (Avesta, Russia); (*3*) second-harmonic generator (Avesta, Russia); (*4*) femtosecond single-pulse autocorrelator ASF-20 (Avesta, Russia); (*5*) cw solid-state laser LCS-DTL-317 (Laser-Export Co. Ltd, Russia); (*6*) cryostat Optistat DN2-V (Oxford Instruments, England) with the sample; (*7*) objective; (*8*) monochromator ML-44 (Solar Laser Systems, Belarus); (*9*) PEM H10720-110 (Hamamatsu, Japan); (*10*) high-speed digital oscilloscope Tektronix DPO4104B; (*11*) high-speed avalanche photodiode SAE500NX (Azimuth-Photonics, Russia); (*12*) computer.

Figure 2 presents the size distribution function of silver ANPs in chloroform.

Laser ablation in chloroform led to the formation of particles with two characteristic sizes; most particles had an average size $r \approx 42$ nm. The nanoparticles were synthesised according to the above-described technique with a laser energy density of ~4.4 J cm^{-2} and a ~30-μm cavity in the silver plate (measured by atomic-force microscopy). Figure 3 shows the absorption spectra of silver ANPs, as well as the luminescence

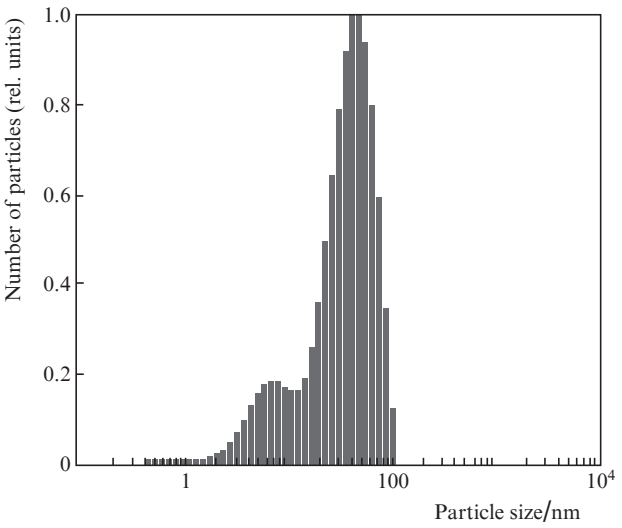

Figure 2. Size distribution function of nanoparticles (produced by laser ablation of silver in chloroform), obtained by means of photon correlation spectroscopy (Photocor-Complex).

(fluorescence and phosphorescence) and absorption spectra of R6G and BG dye molecules in PMMA films.

In the first series of experiments, we investigated the de-excitation of R6G molecules ($C = 5\times10^{-4}$ M) in PMMA at room temperature and upon fluorescence photoexcitation by a femtosecond laser (λ = 516 nm); the fluorescence (λ = 580 nm) and phosphorescence (λ = 690 nm) signals were detected using a PEM and an oscilloscope with an input resistance R = 50 Ω. The inset in Fig. 4 presents a fluorescence oscillogram for R6G in a PMMA film. The oscillogram was processed con-

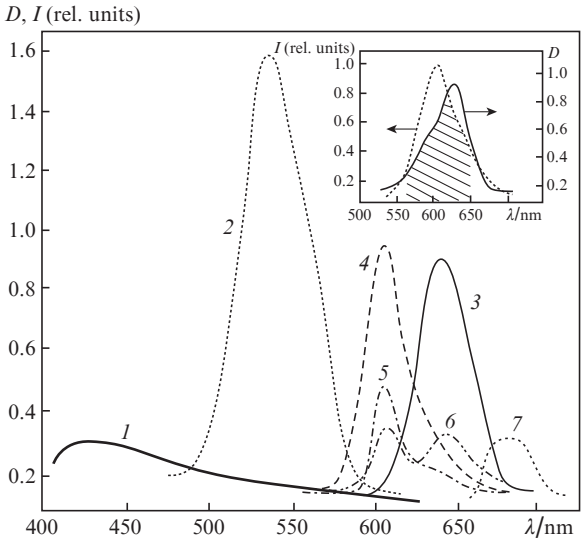

Figure 3. (*1–3*) Absorption spectra of silver ANPs in chloroform [(*1*), $C = 0.85\times10^{-9}$ M] and dyes in PMMA films: R6G [(*2*), $C = 3.1\times10^{-3}$ M] and BG [(*3*), $C = 7.8\times10^{-4}$ M]. (*4–7*) Fluorescence spectra of dyes in PMMA films: R6G [(*4*), $C = 3.1\times10^{-3}$ M], R6G ($C = 3.1\times10^{-3}$ M) and BG ($C = 1.6\times10^{-4}$ M) (*5*), R6G ($C = 3.1\times10^{-3}$ M) and BG ($C = 7.8\times10^{-4}$ M) (*6*), and R6G (*7*). The inset shows the fluorescence spectra of donor (R6G) molecules and absorption spectra of acceptor (BG) molecules.

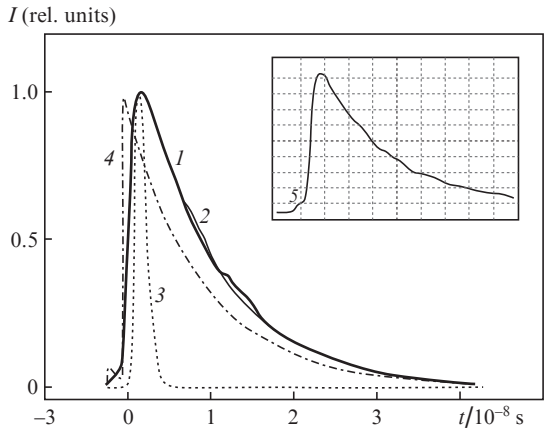

Figure 4. Fluorescence oscillograms of R6G ($C = 5\times10^{-4}$ M) in PMMA and the results of their mathematical processing: (*1*) real fluorescence oscillogram of R6G molecules, (*2*) fitted oscillogram transform, (*3*) instrumental function of the PEM–oscilloscope system, and (*4*) convolution of the instrumental function and signal transform. The inset shows a fluorescence oscillogram of R6G with a hot fluorescence band (*5*).

ventionally: an appropriate exponential transform was chosen for the decay curve and its convolution with the instrumental function of the PEM–oscilloscope system was performed [12]. It can be seen in Fig. 4 that the initial portion of the oscillogram contains a weak peak (*5*), caused by additional luminescence.

Note that this signal arose at excitation intensities below 2.3 GW cm^{-2} or volume excitation energy densities below ~0.357 J cm^{-3} (~3.57×10^6 erg cm^{-3}). The intensity of this luminescence signal is lower than the fundamental luminescence intensity by a factor of ~33.6. One might assign it to 'hot' fluorescence, which was previously revealed and investigated in alcohol solutions of R6G molecules [13]. Photoexcitation of dye molecules into their short-wavelength absorption edge at high excitation intensities provides a quasi-continuous energy distribution over vibrational degrees of freedom [14]. Degradation of the excitation energy of dye molecules involves also vibrational modes of the molecules of the medium, and this exchange with the medium, in contrast to the intravibrational molecular relaxation, may occur with a rate of 10^{10}–10^{11} s^{-1} [13] and depend strongly on the physicochemical structure of the medium (solvent or polymer). Let us estimate the lifetime and nonradiative de-excitation rate of the excited state of the R6G molecule in PMMA at $t = 20$ °C according to the scheme in Fig. 5.

To this end, we will use the formulas [13, 15]

$$\varphi_{fl} = \frac{\tau_{fl}}{\tau_r} = \frac{1}{1 + k_{nr}\tau_r}, \quad (1)$$

$$\tau_{hfl} = \tau_r \varphi_{fl} \frac{I_{hfl}}{I_{fl}}, \quad (2)$$

where φ_{fl} is the quantum fluorescence yield of the dye in PMMA; τ_{fl} and τ_r are, respectively, the fluorescence time and the radiative fluorescence decay time of R6G molecules in PMMA; k_{nr} is the vibrational relaxation rate constant in the singlet excited state; and $I_{hfl}/I_{fl} = 1:33.6$ is the ratio of the hot fluorescence intensity to the intensity of conventional fluorescence.

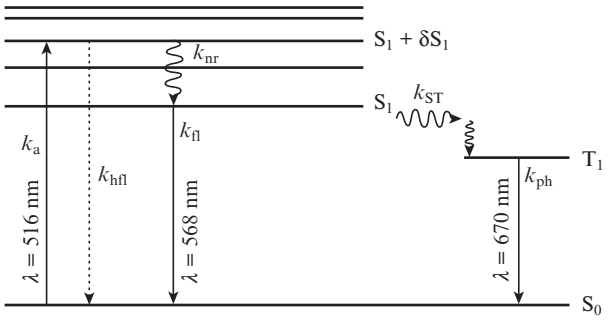

Figure 5. Schematic diagram of electronic transitions in the R6G molecule ($C = 5\times10^{-4}$ M) in PMMA (k_a is the absorption probability, k_{hfl} is the hot-fluorescence probability, k_{nr} is the vibrational relaxation rate constant, k_{fl} is the fluorescence probability, k_{ST} is the intersystem crossing rate constant to the triplet state, and k_{ph} is the phosphorescence probability).

In this study, we used $\varphi_{fl} \approx 0.95$ for R6G in PMMA [7], a value consistent with the results of our measurements. The radiative lifetime of the S_1 state was determined from the oscillator strength of the $S_0 \rightarrow S_1$ transition, found by processing the absorption spectrum of R6G molecules in PMMA: $\tau_r = 5.5\times10^{-9}$ s. Then calculations based on formulas (1) and (2) yield values $k_{nr} \approx 1.5\times10^7$ s^{-1}; $\tau_{hfl} \approx 15\times10^{-11}$ s or $k_{hfl} \approx 0.6\times10^{10}$ s^{-1}, which are very close to the data of [16]. Constant $k_{nr} \approx 10^7$ s^{-1} practically coincides with the intersystem crossing rate constant $k_{ST} \approx 0.34\times10^7$ s^{-1} in an alcohol solution [17]. This fact confirms validity of the condition $\varphi_{fl} + \varphi_T = 1$ (φ_T is the quantum yield of the triplet state) for rhodamine dyes.

Thus, one can observe hot fluorescence of dye molecules in polymer matrices using intense coherent photoexcitation of molecules with a high fluorescence quantum yield, which are fixed in a polymer matrix and, correspondingly, have less free vibrational modes.

It was of interest to analyse the influence of ANPs (added to solution simultaneously with dyes in the stage of preparation of polymer films) on the relaxation processes in PMMA.

An increase in the ANP concentration in PMMA films with R6G molecules led to higher fluorescence and phosphorescence intensities and longer luminescence times: τ_{fl} = 4.94 ns and τ_{ph} = 0.21 ms in the absence of ANPs, whereas τ_{fl} = 5.88 ns and τ_{ph} = 0.22 ms at an ANP concentration of 0.85×10^{-9} mol L^{-1}. The dye fluorescence and phosphorescence times increased by ~18% and ~5%, respectively. One might suggest that the presence of silver nanoparticles changes the structure of a polymer film, as a result of which the rate of relaxation processes in R6G molecules changes due to the violation of settled bonds with the polymer. An alternative explanation of the observed increase in the fluorescence and phosphorescence times of R6G molecules in polymers was given in [9], where this effect was attributed to the rise in the de-excitation rate of excited states of R6G molecules in a polymer under the influence of resonantly excited local surface plasmons in silver nanoparticles.

To reveal the nature of the relaxation processes most strongly affecting the rate of intramolecular degradation of electron energy in dye molecules in PMMA films, both in the presence of silver nanoparticles and in their absence, we performed a spectral and temporal analysis of the fluorescence of R6G molecules in PMMA films in a temperature range from

80 to 330 K. Silver ANPs of different concentrations were introduced into PMMA films. Experiments were carried out in an optical cryostat in vacuum ($P \approx 1\times10^{-5}$ torr) upon photoexcitation of molecules by femtosecond and cw lasers. To exclude possible distortions of spectra at low temperatures due to the formation of dye associates, the R6G concentration was reduced to 5×10^{-5} M.

Cooling films caused a blue shift of peaks in the dye fluorescence spectra and increased the fluorescence time both in the presence of silver nanoparticles and in their absence. The shift value depended on the presence of ANPs in the film. The observed spectral and kinetic changes in the de-excitation of R6G molecules can be due to the α- and β-relaxation processes occurring in the polymer [18] with an increase in temperature up to the PMMA glass-transition point ($T \approx 390$ K) [19]. One of physical causes of the change in de-excitation rates of dye excited states is the acceptance of the oscillation energy of molecular fragments or lateral groups of polymers [20], which contain high-frequency, strongly anharmonic vibrations, for example, vibrations of the C–H group.

Another possible reason for the change in the rate of nonradiative transitions in dye molecules in a polymer film is the break of hydrogen bonds between polymer segments and R6G molecules, which tend to form hydrogen bonds with the medium due to the N–H groups in the R6G structure. In both cases a change in temperature should affect the defreezing of atomic vibrations (γ-relaxation) and atomic groups and fragments (β-relaxation) and the motion of segments and chains (α-relaxation) and, correspondingly, affect the vibrational modes of R6G molecule.

The change in the fluorescence time and the shift of the fluorescence band with a change in temperature in the range of 80–320 K (Table 1) were found to obey an exponential law. Hence, the Boltzmann–Arrhenius formula [18] can be used to describe the vibrational relaxation processes in polymers:

$$\tau_{\text{fl}} = \tau_{\text{fl}}^0 \exp\frac{U}{kT}, \tag{3}$$

where τ_{fl}^0 is the fluorescence time at 80 K and U is the relaxation transition activation energy. To determine U, we analysed the graphical dependences $\ln(\tau_{\text{fl}}/\tau_{\text{fl}}^0) - 1/T$ (method I) and $\ln(\lambda_{\max}/\lambda_{\max}^0) - 1/T$ (method II) for polymers with R6G and ANPs and without silver ANPs. As a result, the following values were obtained: $U^{\text{I}} = 102.83$ cm^{-1} (without ANPs) and 69.44 cm^{-1} (with ANPs); $U^{\text{II}} = 102.1$ cm^{-1} (without ANPs) and 79.42 cm^{-1} (with ANPs).

Table 1. Spectral and kinetic parameters of the fluorescence of R6G molecules ($C = 5\times10^{-5}$ M) in PMMA films containing silver ANPs ($C = 0.85\times10^{-9}$ M).

Temperature/K	τ_{fl}/ns		$\lambda_{\max}$/nm	
	without ANPs	with ANPs	without ANPs	with ANPs
80	3.11	3.69	572	561
130	3.11	3.83	573	562
180	2.90	3.77	573	562
230	3.0	3.53	574	563
280	2.8	3.57	576	564
330	2.7	3.51	576	564

Both methods yield approximately the same activation barrier energies in PMMA films with ANPs, whereas 'defreezing' vibrations somewhat reduce the barrier energy for silver-containing films.

These U values belong to the region of low-frequency librational vibrations of monomeric units in PMMA [21] and correspond to the β-relaxation range. Note that low-frequency vibrations were defrozen in the polymer in our experiments; hence, they cannot be acceptors of the electron energy of excited states of dye molecules [20]. Therefore, the relaxation processes in a polymer film in the temperature range under study vary only slightly. This is confirmed by the fact that the intensity ratio for the hot and conventional fluorescence does not change upon cooling.

Thus, in the presence of silver nanoparticles in a polymer PMMA matrix, the relaxation processes in the nearest environment of R6G molecules change only slightly. A more efficient mechanism is the plasmon-induced increase in the fluorescence intensity and time [9].

It was of interest to investigate the influence of plasmonic interactions on the electron energy transfer in BG–R6G pairs in PMMA films. These experiments were performed on silver ANPs with $r \approx 42$ nm.

Figure 3 demonstrates a strong overlap of the absorption spectra of BG molecules with the fluorescence spectra of R6G molecules in the visible wavelength range. In addition, photoexcitation to the absorption band of R6G molecules is accompanied by generation of surface plasmons in silver ANPs.

The rate constant k_{dd} of nonradiative dipole–dipole excitation energy transfer was calculated in terms of the Forster theory [20]:

$$k_{\text{dd}} = \frac{1}{\tau_{\text{d}}}\left(\frac{R_0}{R}\right)^6, \tag{4}$$

where τ_{d} is the lifetime of the singlet state of donor molecules, R_0 is the critical transfer length, and R is the average distance between donor and acceptor molecules. The distances can be calculated from the formulas

$$R = \sqrt[3]{V/N}, \tag{5}$$

$$R_0 = 0.2108\left[\phi^2\varphi_{\text{fl}}\frac{1}{n^4}\int_0^\infty f(\lambda)\varepsilon(\lambda)\lambda^4\,\text{d}\lambda\right]^{1/6}, \tag{6}$$

where N is the number of particles per volume V;

$$S_{\text{da}} = \int_0^\infty f(\lambda)\varepsilon(\lambda)\lambda^4\,\text{d}\lambda \tag{7}$$

is the overlap integral of the fluorescence spectra of donor (R6G) molecules and the absorption spectra of acceptor (BG) molecules; ϕ is the orientational factor, which amounts to $^2/_3\,0.84$ for solid media; $f(\lambda)$ is the normalised fluorescence spectrum of the donor; λ is the wavelength (nm); n is the refractive index of the medium ($n = 1.7$ for PMMA);

$$\varepsilon(\lambda) = \frac{D(\lambda)}{Cl} \tag{8}$$

is the molar extinction coefficient of acceptor; $D(\lambda)$ is the optical density; C is the concentration (mol L^{-1}); and l is the thickness of the absorbing layer (cm).

The transfer efficiency can be calculated from the formula

$$E^* = 1 - \tau_{da}/\tau_d, \quad (9)$$

where τ_{da} and τ_d are, respectively, the experimental average fluorescence times of donor molecules in the presence and absence of acceptor.

Spectral and kinetic measurements of the energy transfer between R6G ($C = 3.1\times10^{-3}$ M) and BG ($C = 1.6\times10^{-4}$ and 7.8×10^{-4} M) molecules allowed us to calculate the overlap integral of the donor and acceptor wave functions, $S_{da} = 2.4\times10^{15}$ M^{-1} cm^{-1} nm^4; the critical transfer length, $R_0 \approx 4.2$ nm; the average distance between R6G and BG molecules in a PMMA film, $R \approx 7.5$ nm; the dipole–dipole transfer rate constant, $k_{dd} = 0.09\times10^8$ s^{-1}; and the quenching rate constant of excited R6G molecules by BG molecules, $k_q = 1.3\times10^{11}$ M^{-1} L s^{-1}.

The quenching rate constant was calculated from the Stern–Volmer formula:

$$I_0/I_q = 1 + K_{Sh-F}Q, \quad (10)$$

where I_0 and I_q are, respectively, the dye fluorescence intensities in the absence of quenchers (ANPs or BG molecules) and in their presence with a concentration Q; $K_{Sh-F} = k_q\tau'_{fl}$, where k_q is the quenching rate constant by acceptor molecules; and τ'_{fl} is the donor fluorescence time in the absence of transfer and quenching by silver nanoparticles. The values of the corresponding rate constants are listed in Table 2.

Table 2. Kinetic data on the energy transfer between donor (D) molecules (R6G, $C = 3.1\times10^{-3}$ M) and acceptor (A) molecules (BG, $C = 7.8\times10^{-4}$ M) in PMMA films in the presence of silver nanoparticles ($C = 0.85\times10^{-9}$ M).

Dyes in PMMA films	τ_{fl}/ns D/A	E^*	k_{dd}/s^{-1}	k_q/M^{-1} L s^{-1}
R6G	3.3	–	–	–
R6G/BG	3.1/4.1	0.07	0.09×10^8	1.3×10^{11}
R6G/BG + ANPs	1.36/1.42	0.59	0.24×10^8	–

It can be seen in Table 2 that the fluorescence time of R6G molecules decreases with an increase in the acceptor concentration and becomes equal to τ_{fl} for BG in the presence of silver nanoparticles in the film; this behaviour confirms the occurrence of energy transfer in the dipole–dipole pair under study. The fluorescence of R6G molecules is enhanced in the presence of silver ANPs in films with donor–acceptor pairs. The presence of these particles leads also to a significant increase in the electron energy transfer efficiency (by approximately an order of magnitude) and constant k_{dd}.

4. Conclusions

The spectral and kinetic features of the de-excitation of excited states of dye (R6G and BG) molecules in thin PMMA films upon femtosecond and picosecond laser photoexcitation of lower electron states, in the presence and absence of silver nanoparticles obtained by laser ablation in liquid, were investigated. It was found that hot dye fluorescence can be observed in the short-wavelength absorption edge of R6G molecules at high laser pump intensities. The vibrational relaxation time in the R6G molecule and the hot fluorescence lifetime of R6G molecules in the polymer was estimated. Addition of silver nanoparticles to the polymer increases both the fluorescence and phosphorescence times of R6G molecules; this increase is due to the interaction of resonantly excited local surface plasmons in silver nanoparticles with the electron states of R6G molecules. Cooling R6G-containing PMMA films to 80 K made it possible to reveal the relaxation processes in PMMA that are related to librational vibrations of monomeric units in this polymer (corresponding to the β-relaxation range). At the same time, the presence of nanoparticles hardly affects the β-relaxation in the polymer and, therefore, the enhancement or retardation of the nonradiative de-excitation of excited states.

An important result is the observation of almost tenfold increase in the efficiency of nonradiative dipole–dipole energy transfer between R6G and BG molecules in the presence of ablated silver nanoparticles. This increase in the transfer efficiency can be used, e. g., to design light converters for photovoltaic cells.

Acknowledgements. This work was performed within State Contract No. 3.809.2014/K of the Ministry of Education and Science of the Russian Federation.

References

1. Gaponenko S.V. *Introduction to Nanophotonics* (New York: Cambridge University Press, 2010).
2. Bonsak J. *Chemical Synthesis of Nanoparticles for Light Trapping Applications in Silicon Solar Cells* (Oslo: Faculty of Mathematics and Natural Sciences, University of Oslo, 2010).
3. Qian Q., Chong-Xin Sh., Jian Z., Bing-Hui L., Zhen-Zhong Z., De-Zhen S. *J. Lumin.*, **134**, 754 (2013).
4. Boldov I.A., Kuch'yanov A.S., Plekhanov A.I., Orlova N.A., Kargapolova I.Yu., Shelkovnikov V.V. *Fiz. Tverd. Tela*, **53**, 1080 (2011).
5. Protsenko I.E., Uskov A.V., Rudoi V.M. *Zh. Eksp. Teor. Fiz.*, **146**, 265 (2014).
6. Bumai Yu.A., Volubuev V.S., Valeev V.F., Dolgikh N.I., Lukashevich M.G., Khaibullin R.I., Nuzhdin V.I., Odzhaev V.B. *Zh. Prikl. Spektrosk.*, **79**, 781 (2012).
7. Agafonova D.S. *Cand. Diss.* (St. Petersburg, LETI, 2013).
8. Bryukhanov V.V., Tcibulnikova A.V., Samusev I.G., Slezhkin V.A. *J. Appl. Spectrosc.*, **81**, 570 (2014).
9. Bryukhanov V.V., Minaev B.F., Tcibulnikova A.V., Tikhomirova N.S., Slezhkin V.A. *J. Opt. Technol.*, **81**, 7 (2014).
10. El-Bashir S.M., Barakat F.M., AlSalhi M.S. *J. Lumin.*, **143**, 43 (2013).
11. Li X., Fan R., Yu X., Chen D. *J. Lumin.*, **145**, 202 (2014).
12. Lakowicz J.R. *Principles of Fluorescence Spectroscopy* (New York: Springer, 1983).
13. Klochkov V.P., Bogdanov V.L. *Zh. Prikl. Spektrosk.*, **43**, 5 (1985).
14. Rubinov A.N., Richardson M.C., Alcock A.J. *Kvantovaya Elektron.*, **2**, 1681 (1975) [*Sov. J. Quantum Electron.*, **5**, 910 (1975)].
15. Medvedev E.S., Osherov V.I. *Teoriya bezyzluchatel'nykh perekhodov v mnogoatomnykh molekulakh* (Theory of Nonradiative Transitions in Polyatomic Molecules) (Moscow: Nauka, 1983).
16. Bondarev S.L., Knyukshto V.N., Stepuro V.I., Stupak A.P., Turban A.P. *Zh. Prikl. Spektrosk.*, **71**, 179 (2004).
17. Webb J.P., McColgin W.C., Peterson W.C., Stockman D.L., Eberly J.H. *J. Chem. Phys.*, **53**, 4227 (1970).
18. Slutsker A.I., Polikarpov Yu.I., Vasil'eva K.V. *Zh. Tekh. Fiz.*, **72**, 86 (2002).

19. Zakharova O.G., Zaitsev S.D., Semchikov Yu.D. *Dendrimery: sintez, svoistva, primenenie* (Dendrimers: Synthesis, Properties, and Application) (Nizhny Novgorod: NGU, 2006).
20. Ermolaev V.L. *Bezyzluchatel'nyi perenos energii elektronnogo vozbuzhdeniya* (Nonradiative Electronic Excitation Energy Transfer) (Moscow: Nauka, 1977).
21. Ryzhov V.A. *Fiz. Tverd. Tela*, **44**, 2229 (2002).